Dear Paul C. Stoy
Editor Biogeosciences

We acknowledge the opportunity to submit a revised draft of our manuscript. We have implemented most of the suggestions made by the referees. Please see below a point by point response to the referees concerns and the changes made as a consequence of these comments.

Sincerely,
Estefanía Muñoz and Andrés Ochoa

Referee 2

1. Munoz and Ochoa explore patterns of PAR across different latitudes and climate zones. The analysis may be important to the extent that it helps organize and communicate variability in photosynthetically active radiation to the biogeosciences community. At the moment it does not, but I feel that it might. Namely, if the amount of variation in PAR, c, and k explained by solar geometry (obvious) and climate (less obvious) could be determined I could see how obvious aspects of the manuscript could be placed in the context of information that could be quite enlightening for our understanding of how light reaches the surface across the globe. If the authors can do this I feel that the manuscript could be acceptable for publication; at the moment the findings are largely either obvious or unclear, but the latter can be fixed by restructuring the manuscript and explaining more clearly what was done and its implications.

   Author response: We expanded our analysis to also include shortwave radiation. We have now a total of 37 sites. We made figures 3b and 3c to visualize the relation of PDF types with global climate zones and Köppen climate types. Although we analyze radiation, c and k, our main interest is on c and k, not radiation per se. Our important (and less obvious) findings are that:
   a) The PDFs of c and k have the same shape at each site.
   b) We identified three types of PDF: unimodal with low dispersion (ULD), unimodal with high dispersion (UHD), and bimodal (B).
   c) Regionalisation of PDF types can be made by latitude, global climate zones, Köppen climate types, and Holdridge life zones are useful for regionalisation of c and k PDF types. The weakest relation was found for latitude and the stronger for Holdridge life zones (Figs. 3b, 3c and 4).

2. Regarding “Attenuation of light throughout the atmosphere can be calculated by using an attenuation law (e.g. the Beer–Lambert law), but this requires to know the atmospheric optical depth, which is seldom the case” it is also important to note comprehensive atmospheric modeling that seeks to understand the dynamics of atmospheric transmissivity, reflectivity, and absorptivity as a function of wavelength and layer of the atmosphere. Such models are great but difficult to implement at large scales.

   Author response: We wrote the introduction in a more clear form.

3. Page 1 Line 22: light attenuation is not random, it is a function of the physics of the atmosphere.

   Author response: Yes. What is random is the quantity of aerosols and clouds in the atmosphere, not the physics of attenuation. We rewrote the introduction avoiding this misunderstanding.

4. Page 1 Line 25: More evidence is needed that this is the case in the form of references. The Introduction as a whole was a bit too brief. Specifically the notion that c and k are stochastic needs to be addressed in more detail. In many regions, clouds are rather predictable like in areas where sea breezes create weather systems that are easy to anticipate. Fog is another atmospheric phenomenon that is expected and predictable in certain times and certain reasons. I had coastal California ecosystems in mind when writing that but then noted that this paper was published just today. (https://agupubs.onlinelibrary.wiley.com/doi/abs/10.1029/2020GL088428) Please expand the introduction to discuss the variables that change c and k.

   Author response: We enriched the introduction with references reinforcing those statements. We agree on the different tastes of randomness that could occur as a consequence of local/regional climate. We wrote it in a more clear form in the introduction and added a forward reference to the discussion section.

5. Note also that PAR and the shortwave bands overlap, but incompletely. If you are studying PAR, simply explain why and what the important differences are.

   Author response: We expanded our analysis to also include SW radiation.

6. Adding the Holdridge/Koppen zones to Table 1 would be an improvement.

   Author response: We included Table 2 with that information.

7. Why only these 28 sites? There are a number of high-latitude sites with long-term consistent PPFD, for example.

   Author response: These sites were selected from an initial set of more than 200 sites after filtering by several criteria as record length, data quality and spatial coverage of the whole group. We extended our analysis to shortwave radiation. This increased the number of sites to 37. We included this description in the data section.

8. Page 4 Line 6: this is true but requires elaboration: ‘troublesome when using the Beer–Lambert law’. It is certainly troublesome if the atmosphere is considered to be one layer because atmospheric attenuation will vary dramatically by layer over time, but a layer-by-layer implementation of the Beer-Lambert Law over short time scales may be quite accurate but difficult to implement.

   Author response: We included this explanation in the Methods section.

9. After equation 4: ‘transmittance due to molecular absorbers of’: please note that this is for the clean and dry atmosphere for this particular calculation (‘cda’) so that people realize why aerosols and other nonmolecular absorbers (and reflecters) are excluded.

   Author response: We clarified it in the text.

10. Why is forward / back scattering of 0.5 assumed? Please elaborate in the text.

    Author response: Author response: We used 0.5 arbitrarily and expect that the uncertainty and variability of this parameter be expressed in the clarity index (c). We specified this in the text.

11. In equation 5, how much do higher-order reflectances typically contribute? It might not be minor, I'm not sure.

    Although higher reflectances could bring about some subestimation of H, especially during snow-cover periods, we think it is not a critical issue for the sake of this study. Uncertainty caused by these two assumptions will be included in the statistical properties of c.

12. In equation 6, how is ozone derived? Is it weighted for its distribution throughout the atmospheric column? (A simple mean wouldn't do). I note a reference to Iqbal (1983) but elaboration would help the reader.

    Author response: We use the seasonal variation of atmospheric ozone from Iqbal (1983, p.89) that gives the total amount of ozone in a vertical column of air for several latitudes. We interpolate for the latitude and doy of interest. We rewrote this paragraph in a more clear form.

13. Section 3.3: PAR itself is an excellent proxy for cloudiness. Why is precipitation used? Of course it is almost always cloudy when rain is observed but of course more often than not there are clouds but no rain.

    Author response: This is an interesting point deserves an interesting statistical approach, but it is out of our scope in this article. We use rainfall because we have in mind the connection between our statistical characterization of c and k and the ecohydrological and biogeochemical models of Rodríguez-Iturbe and collaborators. That family of models study the stochastic balance equation (for water, carbon, nitrogen) of the soil forced by a Poisson process rainfall model with parameter lambda. We incorporated this context in the introduction and conclusions of the manuscript. We also extended our study to shortwave radiation.

14. Page 6 line 19: Was AT-Neu chosen because it is the first alphabetically? This site is in a north-facing mountain valley and there will be shielding of the sun by mountains to the east and west in the early morning and late afternoon.

    Author response: AT-Neu was selected because it has long and high-quality records. You are right about the local orography at this site. That local trait, as well as the Holdridge life zone or Köppen climate zone, must be reflected in the PDF of c and k.

15. Figures S1 to S28 is a bit too much information, even for a supplement. For Fig. 2C of course there is a 180 day negative autocorrelation because of solar geometry. It is interesting to see that c and k have somewhat more complicated long-term autocorrelation functions but is there a better way to syntheize this than to create 28 figures in a Supplement?

    Author response: We removed the analysis of ACFs.

16. P. 6 L. 22: Too many of these statements are obvious and follow directly from the solar zenith angle and the amount of atmosphere that a beam has to travel through when the sun is not directly overhead. Also, what does this statement mean 'In these sites, climatic seasonality is very weak since the low ACF after removing the astronomical seasonality.' That the statistics of PAR, c, and k are controlled by solar geometry rather than climate? Of course this isn't surprising but it would be interesting to see that proportion of the variables are explained by climate vs. solar geometry, like a variance decomposition. How much of the variability at each site is explained by these two factors and does Koeppen climate classification help explain some of the variability that is not explained by latitude alone?

    Author response: We removed the analysis of ACFs, made the new Table 2 and the new Figures 3 (a, b and c),and improved the design of Figure 4 (Holdridge triangle) to make more clear the analysis of regionalization of c and k.

17. It is still not clear to me what 'bimodal' means. This is a scale-dependent term. More than one peak per day? More than one peak per season?

    Author response: There was an ambiguity with this term. In climatology it means the occurrence of two dry and two wet seasons along the year (common in the tropics), while in statistics it refers to a PDF with two modes. We removed the ambiguity from the text.

18. The statement on page 7 line 9 isn't supported directly by a figure and I am still confused as to what the major objective of the manuscript is**.**

    Author response: Results section was rewrote in a more clear form, including disambiguation of the 'bimodality' concept (see answer to comment 17).

19. P 8: reword: allowing to analyze schematically Does Fig. 4 directed at the notion that some sites have darker clouds than others because of the distributions of c and k on wet and dry days?

    Author response: Results section was rewrote in a more clear form, including disambiguation of the 'bimodality' concept (see answer to comment 17).

20. Figure 5: was a Bonferroni correction applied to significance values? Also, please do not simultaneously use red and green in the same figure. Also, why are both KS and AD tests used? What advantages do they each have and why not choose just one? Are the values in the boxes p-values and why are they frequently greater than 1?

    Author response:
    a) No, we didn't because we are not doing several tests at a time. We test all combinations of pairs of months.
    b) We can change the green/red in Fig. 5.
    c) We used the two tests because AD is more sensitive to the tails of the distribution while KS to the center of the distribution. We clarified this point in the text.
    d) The p-values in the boxes are greater than 1 because they are multiplied by 100 to show more decimals using less space. It will be clarified in the legend of the figure.

21. The paragraph after Figure 5 is confusing (p. 11 line 1). I'm not sure what it means: are the data being used to define when seasons begin and end?

Author response: We are comparing the monthly PDFs of c for the dry-days and wet-days samples to inspect for the existence of c and k seasons (i.e. groups of months where c and k have the same PDF). We wrote it more clearly.

22. Figure 6: Please avoid rainbow color schemes (https://eos.org/features/the-end-of-therainbow-color-schemes-for-improved-data-graphics). Also, the relationship between k and c is merely PAR_0 / PAR_cda. This figure only shows how much atmosphere there is which of course is greater at high latitudes in winter when the sun is arriving at an angle (no idea what is happening with US-SRM). It is an inefficient way of showing the effects of the solar zenith angle on surface radiation.

    Author response: We removed this figure.

23. I cannot emphasize enough how important it is to have very clear subsections when writing a combined Results and Discussion section. The section jumps surprisingly to different topics throughout and is very difficult to follow. Please add subsections at a minimum to help the reader interpret the flow of the argument. I want to very strongly recommend that the analysis have separate Results and Discussions sections to make it easier to follow and to make the importance of the analysis more clear

    Author response: We revised the structure and resolved a problem with Latex. The document is now more clearly structured.

24. Bottom of page 13: I am still not sure what bimodal means in this context and why the analysis is extended to Holdridge life zones. Do some of these ecosystems have expected diurnal or seasonal variability in cloudiness such that grouping the analysis by life zone makes sense?

    Author response: We removed the ambiguity from the text (see answer to comment 17).

25. Also, one would expect that a manuscript submitted to Biogeosciences would discuss the importance of the findings to biogeoscience. In this case the role of PAR in controlling photosynthesis is a logical connection. The paper would be stronger if implications for biogeoscience were discussed in more detail.

    Author response: We included explicit biogeoscientific context in the introduction and conclusions sections.

Referee 3

1. This was an interesting paper about atmospheric attenuation of photosynthetically active radiation (PAR). The paper addresses the spatiotemporal variability in atmospheric attenuation of PAR by analyzing and characterizing the clearness index and the clearday index calculated from long-term observational PAR data for near-globally dispersed sites. The paper provides us with the patterns in atmospheric attenuation of PAR that can be expected for various ecosystems according to their position on the Holdridge triangle or their Köppen climate classification. I enjoyed reading about the indices and the spatiotemporal patterns the researchers have found at a large scale, but the reasons for undertaking the research could be expanded upon.

   Author response: Thank you for your comment. What led us to undertake this research was the need for a probability model of daily radiation to investigate the stochastic dynamics of soil water, nitrogen and carbon contents in energy-limited ecosystems, just as it has been done for water-limited ecosystems (e.g. Ridolfi et al. (2003), Manzoni et al (2004), Botter et al. (2018), Runyan and D'Odorico (2019), Manzoni et al. (2020)). Our ultimate goal is to extend the ecohydrological model of Rodríguez-Iturbe and coauthors from water-limited to energy-limited ecosystems. We are currently working on it (see Muñoz et al. (2020)). We will expand the introduction with this context. We added a final paragraph in the introduction explaining the motivations and importance of our study.

Botter, G., Daly, E., Porporato, A., Rodríguez-Iturbe, I., & Rinaldo, A. (2008). Probabilistic dynamics of soil nitrate: Coupling of ecohydrological and biogeochemical processes. Water Resources Research, 44(3), n/a-n/a. https://doi.org/10.1029/2007WR006108

Manzoni, S., Porporato, A., D'Odorico, P., Laio, F., & Rodriguez-Iturbe, I. (2004). Soil nutrient cycles as a nonlinear dynamical system. Nonlinear Processes in Geophysics, 11(5/6), 589–598. https://doi.org/10.5194/npg-11-589-2004

Manzoni, S., Chakrawal, A., Fischer, T., Schimel, J. P., Porporato, A., & Vico, G. (2020). Rainfall intensification increases the contribution of rewetting pulses to soil respiration. Biogeosciences Discussions, 1--25. https://doi.org/10.5194/bg-2020-95

Muñoz, E., Ochoa, A., Poveda, G., & Rodríguez-Iturbe, I. (2020). Probabilistic soil moisture dynamics of water- and energy-limited ecosystems. EarthArXiv. https://doi.org/10.31223/osf.io/au4tb

Ridolfi, L., D'Odorico, P., Porporato, A., & Rodriguez-Iturbe, I. (2003). The influence of stochastic soil moisture dynamics on gaseous emissions of NO, N2O, and N2. Hydrological Sciences Journal, 48(5), 781–798. https://doi.org/10.1623/hysj.48.5.781.51451

Runyan, C. W., & D'Odorico, P. (2019). Modeling of Phosphorus Dynamics in Dryland Ecosystems. In Dryland Ecohydrology (pp. 309–333). Springer International Publishing. https://doi.org/10.1007/978-3-030-23269-6_12

2. Title: The impression I got from the paper is that it characterizes the site level patterns in atmospheric attenuation that impact how much PAR reaches the ground. The title could be a bit more detailed to include the indices or atmospheric attenuation rather than just "daily PAR".

   Author response: We changed the title to a more precise one.

3. Abstract: The abstract does not communicate why this research was undertaken. The importance of PAR is briefly described in the introduction, but there is no mention of it in the abstract. A sentence about why we should analyze the variability in atmospheric attenuation of PAR in the beginning and another sentence about why the findings or methods are important in the end could help form a complete abstract.

   Author response: We rewrote the abstract in a more clear form.

4. Introduction: At lines 21 and 22, the authors introduce the indices and mention their wide use by other researchers to "quantify the random nature of atmospheric light attenuation" without references to research. The introduction could be expanded to clarify the purpose of studying the variability in atmospheric attenuation of PAR. Some questions below might help expand the introduction: 1. Which studies used the indices to study the variability of atmospheric attenuation? 2. What did those studies find and how does this current research build on previous studies of atmospheric attenuation? 3. Has the variability in the indices been characterized according to climate in the past? If not, why do the authors believe it is important to characterize the variability in atmospheric attenuation by life zone or climate?

   Author response: Thank you for your suggestions. We improved the introduction with references and explaining the random nature of c and k and why we expect to find climatic patterns in their statistical properties.

5. Line 12 on pg 6 mentions that the data was separated into rainy and dry days using precipitation. No precipitation dataset is described in the data section. Adding a description of the source for the precipitation dataset will be helpful.

   Author response: we got rainfall data also from FLUXNET. This was specified in section 2 (Data).

6. Line 18 on pg 6 says: “The time series, annual cycle, and autocorrelogram of PAR, c and k were calculated and plotted for each site.” Is this referring to PAR0 or PARobs?

   Author response: Both. We wrote it in a more clear form. The ACFs were removed.

7. It might be helpful to add that the time series, annual cycle, and autocorrelogram were calculated for PAR in the methods section.

   Author response: We wrote it in the Methods section (ACF analysis was removed).

8. Figure 2 and the corresponding supplementary figures show what appears to be a confidence interval for the ACF with a dotted line. Which level of confidence does that interval mark?

   Author response: It refers to the 95% confidence interval. However, We removed the analysis of ACFs.

9. Figure 2 and figures S1 - S28 need legends with a clarification on which PAR measurement is plotted (PAR0 or PARobs).

   Author response: black solid lines in Figure 2(a,b) indicate the PAR for no-atmosphere and thick green solid lines indicate the modeled global radiation. The thin green solid line in Fig. 2(a) is the time series of the observed PAR and the dots in Fig. 2(b) are the mean of PARobs of each day of the year during the record. We will explain this in the legends or captions of Fig. 2 and Figs. S1-S28.

   Author's changes in manuscript: The legends of Fig. 2 and Figs. S1-S28 were corrected.

10. It is really hard to read the numbers on the figures with the CDF labeled with numbers (figure 5 and figures S57- S84).

    Author response: We changed for symbols instead of numbers.

11. Throughout the paper and figure captions, the parentheses come before the variable they describe. For example: “(a-b) c and (c-d) k”. It is a bit easier to read if the variable is mentioned first: “c (a-b) and k (c-d)”.

Author response: it was corrected.

12. At points in the results/discussion, the figures are introduced by describing the figure. For example: “ Fig. 4 shows the PDFs (left panel) and the CDFs (right panel) for wet (blue) and dry (red) days of c (a–b) and k (c–d).” (Pg. 8, line 17). This seems redundant. A good descriptive caption for the figure or a complete legend should take care of this and the text in the results/discussion does not need to mention it.

Author response: It was corrected.

13. Line 18 on pg. 8 should read: “Figs. S26 to S56 show the results of the 28 sites analyzed.”

Author response: This was corrected.

14. Regarding lines 11 - 14 on pg. 7: “We classified the pdfs of c and k in three types: Bimodal, Unimodal I (unimodal with low dispersion), and Unimodal II (unimodal with high dispersion). Sites in the extratropical northern hemisphere (except the site in the United States US-Fep) have bimodal distributions; sites in tropics, subtropics, and USFpe have Unimodal II distributions; and sites in tropics have Unimodal II distributions.” This appears to be in disagreement with figure 3. US-Fpe looks like it has a Unimodal I distribution in figure 3.

Author response: It was an errata. We corrected it and improved the nomenclature for PDF types and the design of the figure with the Holdridge triangle.

15. If possible, harmonizing the terminology that describes the PDFs between the abstract, results, figures, and conclusion would be helpful. For example, eliminating unimodal I and II altogether and keeping unimodal low and unimodal high to describe the unimodal PDFs throughout the paper and figures should provide consistency for the reader. I also find unimodal low and unimodal high to be more descriptive.

Author response: We improved the nomenclature for PDF types and revised its use in the whole document. The nomenclature is now: unimodal with low dispersion (ULD), unimodal with high dispersion (UHD), and bimodal (B).

16. When talking about the PDFs on pg. 7 and 8: The current organization of paragraphs: Discusses the PDFs’ latitudinal variability on pg. 7 - top of pg. 8, then talks about the Köppen classification, and then talks about the Holdridge triangle with mention of latitudinal variability. Consider moving the paragraph about the Köppen classification (lines 3 - 7, pg. 8) before mentioning the Holdridge triangle and latitudinal variability so that the discussion on the latitudinal variability is continuous. An order such as: Introduce the classification of the PDFs, then discuss Köppen classification of site PDFs, and then discuss Holdridge triangle position and latitudinal variability of site PDF.

Author response: Thank you for your suggestion. We reorganized in a more clear form.

17. What does “NEP-WCMC” stand for on pg 3 line 12?

Author response: We corrected the typing error (“UNEP-WCMC”) and wrote the formal citation: Leemans (1992).

18. There seems to be some disagreement between the abstract and the conclusion. The abstract says: “Unimodal distributions with high dispersion are concentrated in the moist forest life zone in subtropical and tropical regions and humid province; and unimodal distributions with low dispersion are concentrated in dry forest, very dry forest, and thorn woodland in tropical and subtropical regions between arid and subhumid humidity provinces.” The conclusion says: “High latitudes sites exhibit bimodal distributions, arid to sub- humid climates exhibit unimodal distributions with high dispersion, and humid tropical regions exhibit unimodal distributions with low dispersion.”

Author response: Author response: We revised the coherence in the whole manuscript.

~~Bioclimatic~~ Climatic traits ~~in statistical properties of~~ on daily ~~photosynthetically active radiation~~clearness and cloudiness indices

Estefanía Muñoz[1] and Andrés Ochoa[1]

[1]Universidad Nacional de Colombia, Medellín

Correspondence: Estefanía Muñoz (emunozh@unal.edu.co)

Abstract. ~~In this paper, we present a methodology to analyze the stochastic component of daily solar radiation at the earth~~Solar radiation has a crucial role in photosynthesis, evapotranspiration and other biogeochemical processes. The amount of solar radiation reaching the Earth's surface ~~in the photosynthetically active spectral band. Extraterrestrial solar spectral irradiance from the SOLID project and in situ observed PAR from the FLUXNET data set are used to calculate daily time series of the clearness and clear-sky indices for 28 FLUXNET sites around the world for~~ is a function of astronomical geometry and atmospheric optics. While the first is deterministic, the latter has a random behaviour caused by highly variable atmospheric components as water and aerosols. In this study, we use daily radiation data (1978-2014~~. We found that~~) from 37 FLUXNET sites distributed across the globe to inspect for climatic traits in the shape of the probability ~~distribution functions of the clearness and clear-sky indices exhibit a spatial pattern related to the Köppen climate classification and the Holdridge life zones. According to the Köppen classification, oceanic, humid continental, and Mediterranean climates show bimodal distributions; semi-arid, temperate, subtropical, and desert climates show unimodal distributions with high dispersion ; and tropical climates show unimodal distributions with~~ density function (PDF) of the clear-day (c) and the clearness (k) indices. The analysis was made for shortwave radiation (SW) at all sites and for photosynthetically active radiation (PAR) at 28 sites. We identified three types of PDF, unimodal with low dispersion ~~. Moreover, according to the Holdridge triangle, sites with bimodal distributions are concentrated in moist and wet forest life zones located in boreal and cool temperate regions and sub-humid and humid provinces. Unimodal distributions with high dispersion are concentrated in the moist forest life zone in subtropical and tropical regions and humid province; and unimodal distributions with low dispersion are concentrated in dry forest, very dry forest, and thorn woodland in tropical and subtropical regions between arid and subhumid humidity provinces~~(ULD), unimodal with high dispersion (UHD) and bimodal, with no difference in the PDF type between c and k at each site. Looking for regional patterns in the PDF type we found that latitude, global climate zone and Köppen climate type have a weak and the Holdridge life a stronger relation with c and k PDF types. The existence and relevance of a second mode in the PDF can be explained by the frequency and meteorological mechanisms of rainy days. These results are a frame to develop solar radiation stochastic models for biogeochemical and ecohydrological modeling.

1 Introduction

~~Solar irradiation drives~~

Solar radiation drives most physical, chemical and biological processes at the earth's surface. It is the primary energy source ~~of the natural processes of photosynthesisand evapotranspiration (??Hansen, 1999)~~for photosynthesis, evapotranspiration and other biochemical processes (Wu et al., 2016; Mercado et al., 2009). The amount of solar irradiance reaching ~~some~~ any place on the Earth's surface at a given time ~~is the result of~~ results from Sun's emission spectrum, ~~Sun–Earth~~ Sun-Earth distance, the angle of incidence of solar rays, and the atmospheric attenuation of light. The geometry of Earth's orbit and rotation is well-known and can be calculated with high precision. ~~Attenuation of light throughout the atmosphere can be calculated by using an attenuation law (e. g.~~ However, atmospheric attenuation of light is strongly affected by atmospheric constituents such as molecular gases, aerosols, water vapor and clouds by reflecting, absorbing, and scattering processes (Platt et al., 2012; Wallace and Hobbs, 2006). Aerosols, water vapor and clouds are highly variable in space and time. As a consequence, uncertainty is unavoidable when calculating surface solar radiation due to the ~~Beer–Lambert law), but this requires to know the atmospheric optical depth, which is seldom the case~~high space and time variability of aerosols, water vapor and clouds (Li and Trishchenko, 2001; Chen et al., 2000).

~~To affront this problem researchers have relied on statistics.~~ Scientists have affronted the problem of atmospheric light attenuation by mechanistic and statistical approaches. While the former deal with the physical and chemical processes governing light attenuation, the latter use large amounts of observations to infer patterns of variability caused. Two indices are widely used to quantify the random nature of atmospheric light attenuation, the clear-sky index (c) (see Tran, 2013; Harrouni, 2008; Ianetz and Kudish, 2 , defined as the ratio of actual radiation to clean-dry atmosphere radiation, and the clearness index (k) (see Engerer and Mills, 2014; Holland which is the ratio of actual radiation to top-of-the-atmosphere radiation (i.e. with no atmospheric attenuation). Although c and k can be calculated for any spectral band and time aggregation scale, they are often studied at the hourly or daily time steps and for the shortwave band ~~.~~ (e.g. Utrillas et al., 2018; Cañada et al., 2003; Martinez-Lozano et al., 1999). Notice that because of the different physical mechanisms involved in the magnitude, frequency and duration of clouds, water vapor and aerosols across the globe, c and k must show statistical properties related to regional/local climate.

In this paper, we ~~study the bioclimatic traits on the stochastic behavior of daily~~ analyze the statistical properties of c and k ~~for the photosynthetically active radiation (PAR) spectral band. It was possible by using the Solar Spectral Irradiance (SSI)time series, the U. S Standard Atmosphere,~~ at 37 FLUXNET sites distributed worldwide (section 2) looking for climate-related variability patterns. We process historical extraterrestrial spectral irradiance data from the SOLID project (section 2) by using mechanistic models –solar geometry and the Beer–Lambert law (section 3)– to remove the deterministic component of historical daily solar radiation observations. Then, we analyze the probability distribution function of c and ~~observed PAR time series at 28 FLUXNET sites worldwide, distributed in 13 hexagons of the Holdridge triangle (Holdridge, 1947, 1967) corresponding to 8 life zones.~~ k in relation to global climate regions, Köppen climate types and Holdridge life zones (sections 4 and 5).

Characterizing the stochastic behaviour of surface solar radiation is of great importance in many research fields, e.g. photovoltaic electricity generation, photosynthesis, nutrient dynamics in ecosystems, water dynamics in soils and forest fire risks (e.g. Muñoz et al., 2018; Engerer and Mills, 2014). Of special interest are the ecohydrological and biochemical models of (Rodríguez-Iturbe and Porporato, 2004) and collaborators (e.g. Tamea et al., 2011; Laio et al., 2009; Nordbotten et al., 2007; Manzoni et a

, which have had a great progress since the beginnings of the 20th Century. By solving the water balance equation for the rooting soil depth at a daily time-step, they analyze the dynamics of soil moisture (Rodríguez-Iturbe et al., 1999b; D'Odorico et al., 2000; Porporato . In their approach, the water balance equation is a stochastic differential equation forced by the daily rainfall stochastic process. As a result, rainfall probabilistic structure propagates to all other variables of the system. Rodríguez-Iturbe and his coauthors have used this model to study the dynamics of water table depth (Ridolfi et al., 2008; Laio et al., 2009; Tamea et al., 2009), runoff (Botter et al., 2008; Ceola et al., 2010), leaching (Botter et al., 2007), vegetation competition and colonization (Rodríguez-Iturbe et a , soil carbon and nitrogen (D'Odorico et al., 2003; Porporato et al., 2003; Ridolfi et al., 2003; Manzoni et al., 2004), vegetation water stress (Ridolfi et al., 2000; Rodríguez-Iturbe et al., 2001; Laio et al., 2001; Porporato et al., 2001), photosynthesis (Daly et al., 2004a , plant biomass (Schaffer et al., 2015; Nordbotten et al., 2007), waterborne human pathogen invasions (Gatto et al., 2013) and soil related phytopathology (Thompson et al., 2013) in water-controlled ecosystems. All these remarkable works, however, have been oriented to water-limited ecosystems, where uncertainty is introduced by the rainfall process only. To study energy-limited ecosystems, daily solar radiation is required as one more external variable driving evaporation and transpiration processes. Solar radiation is also a random variable, since it highly depends on atmospheric transmittance, specially that of clouds (Muñoz et al., 2020). This paper has the purpose of establishing a framework for daily solar radiation characterization that serves as base for developing the ecohydrology of energy-limited ecosystems.

2 Data

Our data set consists of daily observations of incoming ~~photosynthetic photon flux density (PPFD)~~ solar radiation and rainfall from ~~28~~ 37 sites around the world from the FLUXNET data set (Baldocchi et al., 2001; Olson et al., 2004) (Fig. 1). We analyze two spectral bands, the photosynthetically active radiation (PAR) and the shortwave radiation(SW). While SW observations are available at all sites, PAR observations are available at 28 sites only. Sites have different periods of record spanning from 1996 to 2014 and elevations from sea level to 1550 m (Table 1). These sites were selected from an initial set of more than 200 sites after filtering by several criteria as record length, data quality and spatial coverage of the whole group. FLUXNET PAR data are given as photosynthetic photon flux density (PPFD). The wavelength domain for PPFD in the FLUXNET data set is 400–700 nm (Olson et al., 2004) and has units of μ mol m^{-2} s^{-1}. We convert PPFD to PAR irradiance in W m^{-2} through the relationship 4570 nmol m^{-2} s^{-1}=1 W m^{-2} (Sager and McFarlane, 1997).

We ~~also~~ use the Solar Spectral Irradiance (SSI) at the top of the atmosphere from the "First European Comprehensive Solar Irradiance Data Exploitation project" (SOLID) (Haberreiter et al., 2017; Schöll et al., 2016) as input data for an atmospheric radiation transfer model (section 3). The SOLID spectral time series has a daily time resolution from 1978/7/11 to 2014/12/31 (13204 days) and covers the wavelength range between 0.5 and 1991.5 nm. Data from SOLID are available at http://projects.pmodwrc.ch/solid.

~~The wavelength domain for PPFD in the FLUXNET data set is 400–700 nm (Olson et al., 2004) and has units of $\mu mol\ m^{-2}\ s^{-1}$. We convert PPFD to PAR irradiance in W m^{-2} through the relationship 4570 nmol m^{-2} s^{-1}=1 W m^{-2} (Sager and McFarlane, 1997)~~ .

Table 1. FLUXNET Sites. The record period refers to complete calendar years, i.e. data for all sites start on January 1st of the initial year and end on December 31st of the last year.

Site	Country	Latitude [°]	Longitude [°]	Elevation [m]	Period
AT-Neu	Austria	47.117	11.318	970	2002–2012
AU-DaS	Australia	-14.159	131.388	53	2008–2014
AU-GWW	Australia	-30.191	120.654	486	2013–2014
AU-How	Australia	-12.494	131.152	41	2001–2014
AU-Tum	Australia	-35.657	148.152	1249	2001–2014
BE-Lon	Belgium	50.552	4.746	167	2004–2014
BE-Vie	Belgium	50.305	5.998	493	1996–2014
BR-Sa3	Brazil	-3.018	-54.971	100	2000–2004
CA-Oas	Canada	53.629	-106.198	530	1996–2010
CG-Tch	Congo	-4.289	11.656	82	2006–2009
CH-Oe1	Switzerland	47.286	7.732	450	2002–2008
CH-Oe2	Switzerland	47.286	7.734	452	2004–2014
CN-Cha	China	42.402	128.096	761	2003–2005
CN-Ha2	China	37.609	101.327	3190	2003–2005
CN-HaM	China	37.370	101.180	3250	2002–2004
CN-Qia	China	26.741	115.058	79	2003–2005
DE-Geb	Germany	51.100	10.9143	161.5	2001–2014
DE-Gri	Germany	50.950	13.513	385	2004–2014
DE-Hai	Germany	51.079	10.453	430	2000–2012
DE-Obe	Germany	50.787	13.721	734	2009–2014
DE-Tha	Germany	50.962	13.565	385	1996–2014
GF-Guy	French Guiana	5.279	-52.925	48	2004–2014
GH-Ank	Ghana	5.268	-2.694	124	2011–2014
IT-Lav	Italy	45.956	11.281	1353	2003–2014
IT-MBo	Italy	46.015	11.046	1550	2003–2013
IT-SRo	Italy	43.728	10.284	6	1999–2012
MY-PSO	Malaysia	2.973	102.306	~~148~~ 147	2003–2009
PA-SPs	Panama	9.314	-79.631	68	2007–2009
RU-Fyo	Russia	56.461	32.922	265	1998–2014
SD-Dem	Sudan	13.283	30.478	500	2005–2009
SN-Dhr	Senegal	15.403	-15.432	40	2010–2013
US-Bn2	USA	63.920	-145.378	410	2002–2004
US-Esm	USA	25.438	-80.595	1.07	2008–2014
US-FPe	USA	48.308	-105.102	634	2000–2008
US-NC2	USA	35.803	-76.668	5	2005–2010
US-SRM	USA	31.821	-110.866	1120	2004–2014
ZA-Kru	South Africa	-25.020	31.497	359	2009–2013

~~Information of~~ In order to analyze the spatial climatic patterns of the random component of PAR and SW radiation, we use the Köppen climate classification ~~and~~ from Peel et al. (2007), downloaded from the author's webpage and the Holdridge life zones ~~is taken from Rubel and Kottek (2010) and NEP-WCMC, respectively~~(Holdridge, 1947, 1967) from Leemans (1992), downloaded from UNEP-WCMC.

3 Methods

Daily radiation amount at a site on the earth's surface is the result of integrating instantaneous irradiance over the day length. Surface instantaneous irradiance estimation comprises solar irradiance at the top of the atmosphere (TOA) and the physical properties of the atmosphere for the site and time of interest. We use SOLID data for TOA irradiance and the Beer–Lambert law to calculate light attenuation by the atmosphere (see details in section sec:Hcda). However, some atmospheric components

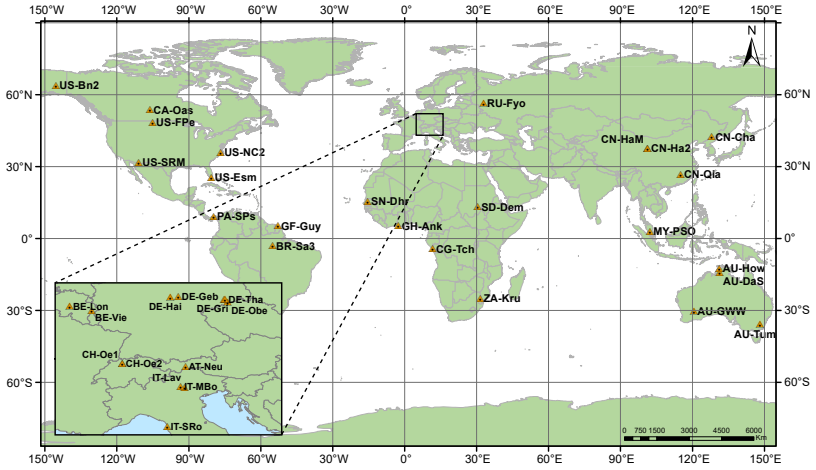

Figure 1. The sites selected from the FLUXNET dataset are spanned over several continents and climates.

as clouds, water vapor, and aerosols are highly variable in space and time, which is troublesome when using the Beer–Lambert law for a one-layer atmosphere. Therefore, we follow two approaches: 1) use the clear-day index (c) (also known as relative clearness index, clear day index, and normalized clearness index) to assess the effect of the variable components on total daily radiation, and 2) use the clearness index (k) to assess the whole atmospheric effect on total daily radiation. Both indices are defined in Eqs. (1), where ~~PAR_{obs}~~ H_{obs} is the observed daily global ~~PAR~~ radiation on a horizontal surface at the ground level, ~~PAR_0~~ H_0 is the extraterrestrial daily global ~~PAR~~ radiation on a horizontal surface, and ~~PAR_{cda}~~ H_{cda} is the daily global ~~PAR~~ radiation on a horizontal surface on the ground for a cloudless, clean, and dry atmosphere.

$$c = \frac{PAR_{obs}}{PAR_{cda}} \frac{H_{obs}}{H_{cda}}, \quad k = \frac{PAR_{obs}}{PAR_0} \frac{H_{obs}}{H_0} \tag{1}$$

3.1 ~~PAR~~ Daily radiation at the top of the atmosphere

~~Photosynthetically active radiation at the top of the atmosphere (PAR_0) is calculated by integrating the~~ Integration of the daily SSI over the ~~PAR spectral band~~ spectral band of interest (400–700 nm ~~) to obtain~~ for PAR, 285–280 nm for SW) gives the Total Spectral Irradiance for each band (TSI_{PAR} ~~)~~and TSI_{SW}) at TOA, as shown in Eq. (~~??)and doing the~~ 2). After some geometric transformations accounting for solar declination (δ) and latitude (ϕ) ~~,~~ (Iqbal, 1983), the daily globla radiation on a horizontal surface can be calculate as shown in Eq. (~~??)(Iqbal, 1983).~~ 3).

$$TSI_{PARBand} = \int_{400\ nm_{Band}}^{700\ nm} SSI\, \mathrm{d}\lambda \tag{2}$$

$$PARH0_0 = \frac{24E_0}{\pi} TSI_{PARBand} (\omega_{sr} \sin\delta \sin\phi + \cos\delta \cos\phi \sin\omega_{sr}) \tag{3}$$

where E_0 is the eccentricity correction factor of the earth's orbit and ω_{sr} is the sunrise hour angle for the day.

3.2 ~~Surface PAR~~ Daily surface radiation for a cloudless, clean dry atmosphere

~~Surface PAR~~ Daily surface radiation for a cloudless, clean, and dry atmosphere (~~PAR_{cda}~~ H_{cda}) is the sum of the direct (~~PAR_b~~ H_b) and diffuse (~~PAR_d~~ ~~components~~ (~~$PAR_{cda} = PAR_b + PAR_d$~~) H_d) components. To calculate daily ~~PAR_b~~ ~~and~~ ~~PAR_d~~ H_b and H_d on a horizontal surface at the ground level, we model the direct and diffuse instantaneous spectral irradiances and integrate them along the day length and the PAR ~~spectral domain.~~ and SW spectral domains.

Following Iqbal (1983), we assume the cloudless, clean and, dry atmosphere to be composed by uniformly mixed gases (m) and ozone (o). Using the Beer–Lambert law and integrating, daily ~~PAR_b~~ H_b is calculated as in Eq. (4).

$$PARR_b = \int_{\gamma_{sr}}^{\gamma_{ss}} \int_{\frac{400\ nm}{700\ nm}Band} SSI_{0,n,\lambda} E_0 \sin(\gamma) \tau_{ma,\lambda} \, \mathrm{d}\lambda \, \mathrm{d}\gamma \tag{4}$$

where $SSI_{0,n,\lambda}$ is the extraterrestrial spectral irradiance normal to the rays from the sun (obtained from SOLID), γ is the solar altitude varying from sunrise (sr) to sunset (ss), and $\tau_{ma,\lambda}$ is the transmittance due to the molecular absorbers of the cda atmosphere.

For the assumed atmosphere composition $\tau_{ma,\lambda} = \tau_o \cdot \tau_g$, where τ_o and τ_g are the ozone and the mixed gases transmittance, respectively (see details in Iqbal, 1983, Sec.6.14). ~~Assuming~~ We arbitrarily assumed forward and backward scatterances of 0.5 and ~~considering~~ considered only the first pass of radiation through the atmosphere~~, PAR_d can~~. Although higher reflectances could bring about some subestimation of H, especially during snow-cover periods, we think it is not a critical issue for the sake of this study. Uncertainty caused by these two assumptions will be included in the statistical properties of c. H_d can then be calculated by

$$PARH_d = \int_{\gamma_{sr}}^{\gamma_{ss}} \int_{\frac{400\ nm}{700\ nm}Band} SSI_{0,n,\lambda} E_0 \sin(\gamma) \tau_{ma,\lambda} [0.5(1 - \tau_{r,\lambda})] \, \mathrm{d}\lambda \, \mathrm{d}\gamma \tag{5}$$

where $\tau_{r,\lambda}$ is the transmittance due to Rayleigh molecular scattering (see details in Iqbal, 1983, Sec.6.14).

Several atmospheric parameters are required by Eqs. (4) and (5). We assume the 1976 U.S. standard atmosphere (NASA, 1976) (sea level pressure of 101.325 kPa, sea level temperature of 288 K, and sea level density of 1.225 kg/m^3) and the Kasten and Young (1989, Table II) optical air mass function of solar altitude, which has 336 values for solar altitudes between 0°and 90°. Transmittance for ozone and mixed gases are calculated as in Eqs. (6) to (8).

$$\tau_{o,\lambda} = \exp(-k_{o,\lambda} l_o m_r) \tag{6}$$

$$\tau_{g,\lambda} = \exp\left[\frac{-1.41 k_{g\lambda} m_a}{(1 + 118.93 k_{g\lambda} m_a)^{0.45}}\right] \tag{7}$$

$$\tau_{r,\lambda} = \exp(0.008735\lambda^{-4.08} m_a) \quad (8)$$

where m_r is relative air mass at standard pressure, m_a is relative air mass at actual pressure, k_o and k_g are the absorption attenuation coefficient for oxygen and mixed gases, and l_o is the amount of ozone in cm (at normal temperature and pressure, NTP). We calculate $k_{o,\lambda}$ for any λ value using the Leckner (1978) interpolation of the classic Vigroux (1953) data. For calculating l_o we interpolate, for each latitude and doy of interest, the Table 5.3.2 from Iqbal (1983) ~~, which~~ which gives the monthly total amount of ozone in a vertical column of air for several latitudes. Table 5.3.2 from Iqbal (1983) is a reproduction of Robinson (1966, p.114). $k_{o,\lambda}$ is calculated by interpolating Table 6.13.1, which is a reproduction of Table 4 in Leckner (1978, p.146).

3.3 Statistical properties of k and c

~~We estimate the~~ After the process described is sections 3.1 and 3.2, we calculated daily time series ~~, annual cycles, autocorrelograms,~~ of c and k by using the expressions in Eq. (1) for the SW and PAR spectral bands. Then, we estimated the mean annual cycle, and empirical probability density functions (PDF) of H, c, and k for both bands. We separate the data samples of c and k by ~~rainy~~ humid and dry days, using precipitation data as a proxy of cloudiness and water vapor in the atmosphere. Then, we inspect the seasonality of c and k by comparing the cumulative distribution function (CDF) of each month with the CDFs of the other months. The comparison of the CDFs is carried out visually and tested by using Kolmogorov–Smirnov (KS) and Anderson–Darling (AD) Goodness of Fit Tests (Dodge, 2008; Pearson, 1900; Scholz and Stephens, 1987). We use both tests because AD is more sensitive to the tails KS to the center of the distribution.

4 Results~~and Discussion~~

The time series ~~, annual cycle , and autocorrelogram of PAR~~ and the mean annual cycle of PAR and SW, c and k were ~~calculated and plotted for each site. The results for AT-NEU are shown in Fig. 4, and those for all other sites are in Figs. S1 to S28. Notice that some values of c and k are greater than 1 during winter in sites with seasonal snow. This anomaly can be explained by the multiple reflection of light enhanced by the snow cover.~~

~~Time series, annual cycle, and autocorrelation function of PAR (a–c), c (d–f), and k (g–i) at AT-Neu.~~

~~The autocorrelograms of PAR, c, and k indicate a more marked annual cycle for PAR than for c and k (see~~ plotted for all sites. Since these are so many figures, they are put in the Supplementary Material. The case of AT-Neu, a site with long and high-quality records, is shown in Fig. 4~~), except at most of the tropical sites (BR-Sa3, CG-Tch, GF-Guy, GH-Ank, MY-PSO, PA-SPs, SD-Dem, and ZA-Kru). All tropical sites have a very weak autocorrelation function (ACF), while extratropical sites show strong ACFs of PAR. Clearness and clear-sky indices remove the astronomical seasonality, indicating that PAR seasonality in extratropical sites is almost entirely explained by the astronomical seasonality. The above is pointed out by the weaker ACFs of k and~~ . A seasonal pattern is observed in the maximum values along the year, but c ~~when compared with the ACF of PAR. In these sites, climatic seasonality is very weak since the low ACF after removing the astronomical seasonality. In~~

contrast, tropical sites show a seasonality almost completely explained by the climatic seasonality (and not by the astronomical seasonality), being the ACF of the indices and PAR very similar.

The ACF of and k is stronger than that of c in most sites (take values spanning over their whole domain. Splitting the data in two samples, the rainy days and dry days, allowed the estimation of the PDFs and CDFs. As shown in Fig. 4, panels f and i).The calculation of k does not include any atmosphere, while c considers a cloudiness-sky, clean, and dry atmosphere. The high ACFs of k suggest that the atmosphere (specifically the air mass) has seasonality, that k does not manage to remove (Ianetz and Kudish, 2008).

ACFs show a period of 180 days approximately for all the sites studied, except in BR-Sa3 where it is 120 days (for both PAR and the indices), and in 3, AT-Neu where it is 80 days (only for the indices). As seasonality depends largely on the movement of the sun, the periods in sites nearest to the geographical Equator should be shorter than those of extratropics, as in BR-Sa3. However, seasonality is also a functionof local factors not dealt with in this paper. The differences in the periods of PAR and its indices in AT-Neu can be explained because the climatic and astronomical seasonalities are out of phase.

The pdfs of c and k reveal a certain degree of bimodality, or at least, some asymmetry in respect to the mean, as mentioned before by Hollands and Suehrcke (2013); Tovar-Pescador (2008); Assunção et al. (2003); Ibánez et al. (2003); Jurado et al. (1995); Skartv (see Fig. S29 to S56). We classified the pdfs of c and k in three types: Bimodal, Unimodal I (unimodal PDFs have a bimodal shape (i.e. a PDF with two modes). Inspection of the PDFs of all sites motivated us to define three types of PDF according to the shape of the function. We propose the following PDF type: Unimodal with low dispersion), and Unimodal II ((ULD), unimodal with high dispersion). Sites in the extratropical northern hemisphere (except the site in the United States US-Fep) have bimodal distributions; sites in tropics, subtropics, and US-Fpe have Unimodal II distributions; and sites in tropics have Unimodal II distributions. The same behavior is observed for k (UHD) and c. This led us to suspect that k and c follow bimodal distributions in high latitudes, unimodal distributions with high dispersion in mid-latitudes, and unimodal distributions with low latitudes.

Looking for spatial patterns in the PDF shapes of daily c and k, we arranged sites following the Köppen classification and Holdridge life zones (Holdridge, 1947, 1967). According to the Köppen classification, bimodality occurs in oceanic, humid continental, and Mediterranean climates; unimodal PDFs with high dispersion in tropical monsoon, tropical savanna, and tropical rainforest climates; and unimodal PDFs with low dispersion in semi-arid, temperate, subtropical humid, and desert climates.

The Holdridge life zones triangle has the advantage of allowing to analyze schematically the link between climate and long-term behavior of c and k. Red symbols in bimodal (B) (see a graphical description in Fig. 6 represent the sites with bimodal PDFs of k and c, purple symbols the sites with unimodal I PDFs, and yellow symbols the sites with unimodal II PDFs. Bimodality is concentrated in moist and wet forest life zones in the cool temperate and boreal regions on subhumid and humid provinces. Sites in moist and wet forest life zones in humid tropical and subtropical regions on the humid province have Unimodal II distributions, and sites dry forest, very dry forest, and thorn woodland life zones have Unimodal I distributions. The latter are in the tropical and subtropical regions on humidity provinces between arid and subhumid. Although US-Fpe has Unimodal I PDF and is located in the cool temperate region, it stays in the same range of humidity provinces as the other sites

with this type of PDF (i.e., arid to subhumid). Fig. 6 allows us to infer the high influence of latitude and the type of climate on the statistical behavior of c and k. 5a).

After separating data by rainy and dry days, we divided them by months to define the seasons of the indices. c and k, i.e., groups of months where the indices have the same PDF. These definition was performed observing the aggregation of the monthly CDFs and comparing the CDF of each month with the those of the other months with KS and AD Goodness of Fit Tests. Fig. 4 shows the CDF of each month separated by rainy (blue lines) and dry (red lines) days(a–b)and dry days, and the comparison matrices of the PDF of each month (c–j) at the AT-Neu site. Values into cells are the p-values obtained with KS and AD Goodness of Fit Tests. Figs. S57 to S84 show the results of all sites studied. The definition of index separation of seasons is very clear in the extratropical sitessince the CDFs of months with low values of c and k are notoriously thrown to the left side, and the months with high values to the right side, both for rainy and dry days (see Fig. 4(a–b)). Besides, the matrices of comparison corroborate it. Nevertheless, at sites within or near the tropics, the , while in tropical sites monthly CDFs are not markedly clearly grouped, and matrices of comparison do not indicate clear seasons. similar behavior among months. AD method results in more clearly defined seasons and with more months that the KS method, suggesting that the most important differences occur in the center of distributions (where KS is more sensitive).

At most sites, it is possible to define two seasons: Season 1 (Season 2) includes the period in which high (low) values of k and c are more likely. In the extratropical northern hemisphere, Season 1 (Season 2) occurs approximately between November (March) and February (September). We notice that at many sites there is a transition between seasons, but it is not considered here. Furthermore, at most tropical sites, there is no precise differentiation of seasons.

The beginning and the end of seasons do not change notably with the index (k and c), but they do with the occurrence or non-occurrence of rainfall. Only at IT-MBo, US-Esm and US-NC2, they do not change. At the other sites, season 1 is usually shorter than season 2 for dry days, and longer than season 2 for rainy days. When analyzing the changes in the beginning and the end of the seasons according to the Holdridge life zones, we do not observe clear patterns. This may indicate that local factors control when the seasons of the indices begin and end.

Fig. **??** shows the relationship between the clearness and the clear-sky indices. The graphics are sorted in descending order of latitude, and each color dot indicates a month. Black dots represent the days in January, green dots the days in July, and red dots the days in December.From Eqs. (1

Looking for climate-related regionalization patterns, the c and k PDF type was compared to the global climate region (Fig. 5b), the slope of lines (m) is given by PAR_0/PAR_{cda}. As PAR_0 does not consider the absorption by atmosphere components, it has a higher value than PAR_{cda} that does it, being m always greater than 1. Sites in high northern latitudes show a notable variability of m throughout the year, while in the tropics and the southern hemisphere, the dispersion is very low.

Köppen climate classification (Fig. **??** shows the daily eccentricity correction factor (E_0) (orange line) and the relative air mass (purple lines)for different latitudes. E_0 denotes the Sun–Earth distance for any day of 5c) and the year, indicating the potential energy arriving at the Earth's surface when there is no atmosphere. In the extratropical latitudes, m_a has a great variation, while in the tropics it is almost constant (dotted line) . The changes in m_a explain the high dispersion of m in high

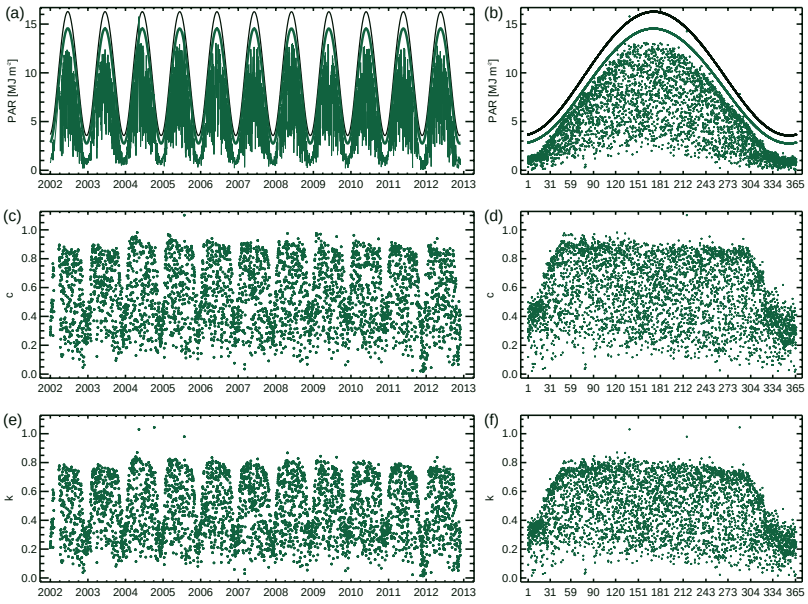

~~Fig. 3 shows the PDFs (left panel) and the CDFs (right panel) for wet (blue) and dry (red) days of c~~ PAR (a–b~~) and k~~), c (c–d~~). Figs. 26 to 56 show the results of the 28 sites analyzed. Because bimodality is attributed to clear and overcast sky conditions (Tovar-Pescador, 2008; Olseth and Skartveit, 1984), by separating the values of c~~), and k ~~on rainy and dry days, bimodal PDFs are divided into two unimodal ones, except for~~ (e–f) at AT-Neu. Solid black and green lines in panels (a) and (b) indicate PAR_0 (no atmosphere), ~~DE-Geb, and DE-Hai, where the PDFs of dry days continue to have a bimodal distribution. This can be explained by the presence and absence of clouds on dry days since there is not always a direct relationship between rainfall and clouds.~~ and PAR_{cda} (clean and dry atmosphere), respectively. Thin lines in (a) and points in (b) show PAR_{obs}.

~~Fig. 3 shows the PDFs (left panel) and the CDFs (right panel) for wet (blue) and dry (red) days of c~~ PAR (a–b~~) and k~~), c (c–d~~). Figs. 26 to 56 show the results of the 28 sites analyzed. Because bimodality is attributed to clear and overcast sky conditions (Tovar-Pescador, 2008; Olseth and Skartveit, 1984), by separating the values of c~~), and k ~~on rainy and dry days, bimodal PDFs are divided into two unimodal ones, except for~~ (e–f) at AT-Neu. Solid black and green lines in panels (a) and (b) indicate PAR_0 (no atmosphere), ~~DE-Geb, and DE-Hai, where the PDFs of dry days continue to have a bimodal distribution. This can be explained by the presence and absence of clouds on dry days since there is not always a direct relationship between rainfall and clouds.~~ and PAR_{cda} (clean and dry atmosphere), respectively. Thin lines in (a) and points in (b) show PAR_{obs}.

Figure 2. ~~Holdridge's life zones triangle. The 28 FLUXNET sites~~ Time series and annual cycle of ~~this study are distributed in 13 hexagons corresponding to 8 life zones.~~

~~Fig. 3 shows the PDFs (left panel) and the CDFs (right panel) for wet (blue) and dry (red) days of c~~ PAR (a–b~~) and k~~), c (c–d~~). Figs. 26 to 56 show the results of the 28 sites analyzed. Because bimodality is attributed to clear and overcast sky conditions (Tovar-Pescador, 2008; Olseth and Skartveit, 1984), by separating the values of c~~), and k ~~on rainy and dry days, bimodal PDFs are divided into two unimodal ones, except for~~ (e–f) at AT-Neu. Solid black and green lines in panels (a) and (b) indicate PAR_0 (no atmosphere), ~~DE-Geb, and DE-Hai, where the PDFs of dry days continue to have a bimodal distribution. This can be explained by the presence and absence of clouds on dry days since there is not always a direct relationship between rainfall and clouds.~~ and PAR_{cda} (clean and dry atmosphere), respectively. Thin lines in (a) and points in (b) show PAR_{obs}.

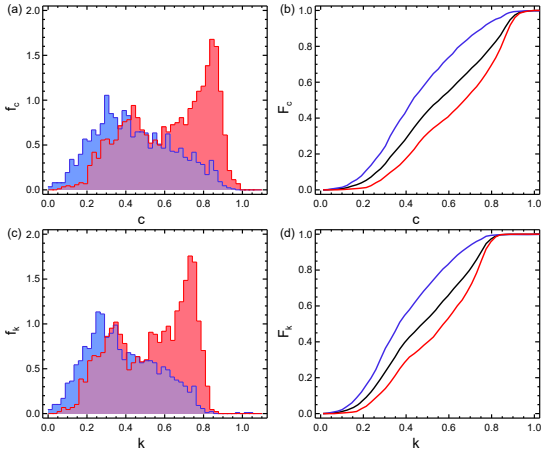

Figure 3. PDFs (left panel) and CDFs (right panel) for ~~wet~~ rainy (blue) and dry (red) days of c (a–b) ~~e~~ and k (c–d) ~~k~~ for PAR at AT-Neu FLUXNET site.

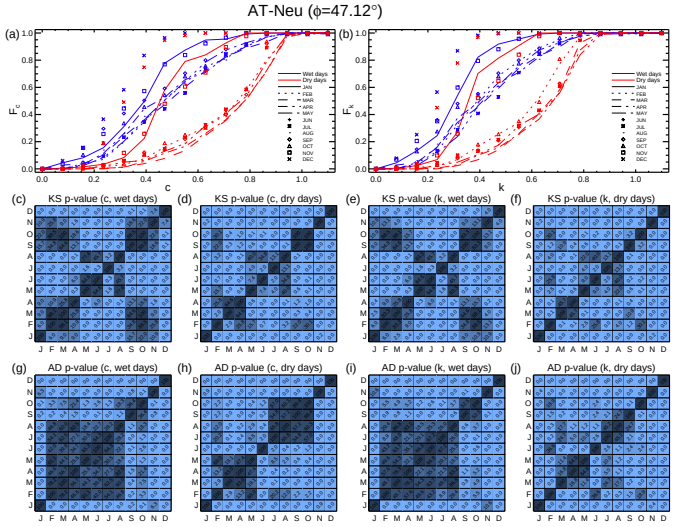

Figure 4. Monthly CDFs of c (a)~~e~~, and k (b)~~k~~. ~~(c–j)~~ p-value of the 2-sample KS and AD tests applied to all combinations of monthly CDF of c and k during wet (blue) and dry (red) days at AT-Neu (c–j). p-values are multiplied by 100 to show more decimals using less space.

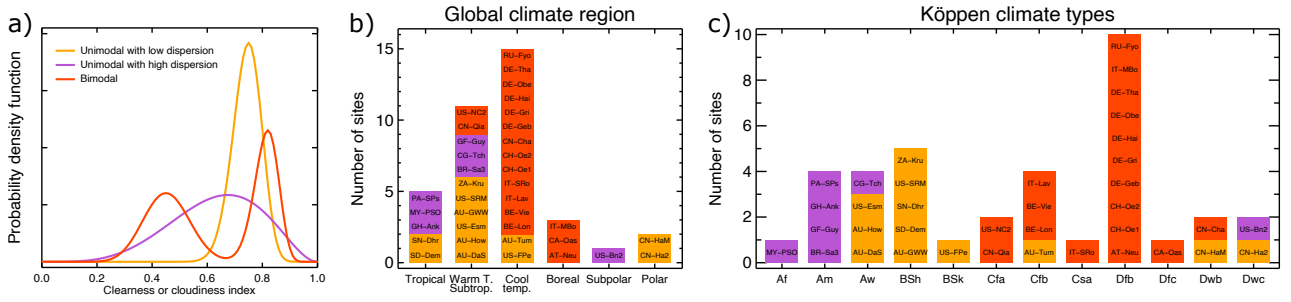

Figure 5. ~~Relationship between~~ Panel a) shows a scheme of the three PDF types of k and c. ~~Graphs are sorted by decreasing latitude from~~ Panels b) and c) show the ~~top-left to the bottom right. Colors indicate the day~~ climatic distribution of the ~~year (doy)~~identified PDF types for the 37 case studies.

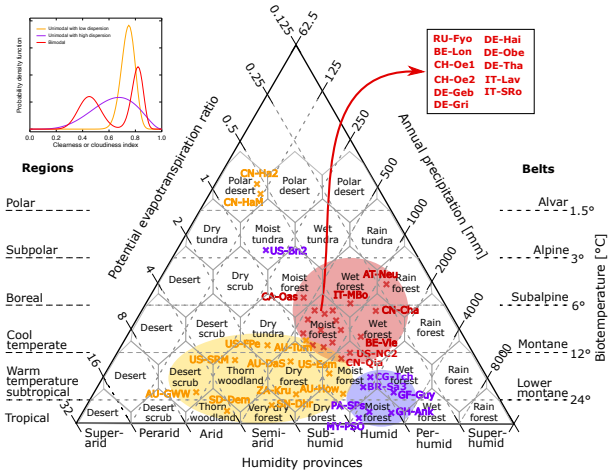

Figure 6. ~~Daily variability~~ Plotting all sites in the Holdridge's life zones triangle shows three groups of ~~eccentricity correction factor~~ sites with the same c and ~~optical mass for several latitudes~~k PDF shape. Red symbols represent bimodal, purple symbols unimodal with high dispersion and yellow symbols unimodal with low dispersion PDFs.

~~latitudes and the low dispersion at sites near the equator. In northern high latitudes, the largest differences between c and k occur at the beginning and the end of the year since the path length that light rays must pass through is longer than in the middle of the year~~Holdridge life zones (Fig. 6). An in-depth inspection of the plots of all sites allowed to set out the following statements: a) the same behavior is observed for c and k at each site, b) latitude is not enough to explain the shape of the PDFs, c) Köppen climate types show a more clear pattern than global climate regions, d) Holdridge life zones show the clear cut pattern of variability of the PDF types. Table 2 summarizes these results and the Köppen and Holdridge classification of each site.

Table 2. Climate classification and k and c PDF type of all sites. Table is sorted by decreasing latitude.

Site	Latitude [°]	Global Climate Region	Köppen climate type	Holdridge Life Zone	PDF Type
US-Bn2	63.920	Subpolar	Dwc	Alpine Moist tundra	UHD
RU-Fyo	56.461	Cool temperate	Dfb	Montane Moist forest	B
CA-Oas	53.629	Boreal	Dfc	Subalpine Moist forest	B
DE-Geb	51.100	Cool temperate	Dfb	Montane Moist forest	B
DE-Hai	51.079	Cool temperate	Dfb	Montane Moist forest	B
DE-Tha	50.962	Cool temperate	Dfb	Montane Moist forest	B
DE-Gri	50.950	Cool temperate	Dfb	Montane Moist forest	B
DE-Obe	50.787	Cool temperate	Dfb	Montane Moist forest	B
BE-Lon	50.552	Cool temperate	Cfb	Montane Moist forest	B
BE-Vie	50.305	Cool temperate	Cfb	Montane Wet forest	B
US-FPe	48.308	Cool temperate	BSk	Montane Dry tundra	ULD
CH-Oe1	47.286	Cool temperate	Dfb	Montane Moist forest	B
CH-Oe2	47.286	Cool temperate	Dfb	Montane Moist forest	B
AT-Neu	47.117	Boreal	Dfb	Subalpine Rain forest	B
IT-MBo	46.015	Boreal	Dfb	Subalpine Wet forest	B
IT-Lav	45.956	Cool temperate	Cfb	Montane Moist forest	B
IT-SRo	43.728	Cool temperate	Csa	Montane Moist forest	B
CN-Cha	42.403	Cool temperate	Dwb	Montane Wet forest	B
CN-Ha2	37.609	Polar	Dwc	Alvar Polar desert	ULD
CN-HaM	37.370	Polar	Dwb	Alvar Polar desert	ULD
US-NC2	35.803	Warm temperate/Subtropical	Cfa	Lower montane Moist forest	B
US-SRM	31.821	Warm temperate/Subtropical	BSh	Lower montane Thorn woodland	ULD
CN-Qia	26.741	Warm temperate/Subtropical	Cfa	Lower montane Moist forest	B
US-Esm	25.438	Warm temperate/Subtropical	Aw	Lower montane Moist forest	ULD
SN-Dhr	15.403	Tropical	BSh	- Very dry forest	ULD
SD-Dem	13.283	Tropical	BSh	- Thorn woodland	ULD
PA-SPs	9.314	Tropical	Am	- Moist forest	UHD
GF-Guy	5.279	Warm temperate/Subtropical	Am	Lower montane Wet forest	UHD
GH-Ank	5.268	Tropical	Am	- Moist forest	UHD
MY-PSO	2.973	Tropical	Af	- Moist forest	UHD
BR-Sa3	-3.018	Warm temperate/Subtropical	Am	Lower montane Moist forest	UHD
CG-Tch	-4.289	Warm temperate/Subtropical	Aw	Lower montane Moist forest	UHD
AU-How	-12.494	Warm temperate/Subtropical	Aw	Lower montane Dry forest	ULD
AU-DaS	-14.159	Warm temperate/Subtropical	Aw	Lower montane Dry forest	ULD
ZA-Kru	-25.020	Warm temperate/Subtropical	BSh	Lower montane Dry forest	ULD
AU-GWW	-30.191	Warm temperate/Subtropical	BSh	Lower montane Desert scrub	ULD
AU-Tum	-35.657	Cool temperate	Cfb	Montane Moist forest	ULD

5 ~~Conclusions~~Discussion

We analyzed the stochastic behavior of the daily clearness and clear-sky indices for the ~~photosynthetically active spectral domain~~PAR and SW spectral domains. Both indices remove the astronomical seasonality, and c also removes the seasonality of the clean and dry air optical mass. Therefore, c is neater than k in describing the effect of the highly variable components of the atmosphere, i.e., clouds, water vapor, and aerosols.

Due to the multiple ~~refractions~~ reflections of light by snow, we found a few values of c and k greater than 1 in sites where there is seasonal snow, during the periods in which it occurs ~~.~~

(e.g. AT-Neu, Fig. 4). This could introduce important errors if we were performing a forecast work, but it is not so problematic in this study. The analysis of rainy and dry days revealed that c and k have ~~similar statistical shape PDFs as indicated by Escobedo et al. (2009), but k exposed higher values than c. The differences between c and k are more accentuated in the~~

~~extratropical northern hemisphere since the path length that energy must pass through varies considerably during the year. Besides, in~~ the same PDF shape for both indices at each site. This result is obvious because the whole data sample was separated by rainy and dry days and both indices are designed to take into account the effect of water in the atmosphere. This is also a reason explaining that the ~~extratropical northern hemisphere,~~ PDF shows the same shape type for the SW and the PAR bands.

Although radiation itself is a proxy of cloudiness (Nyamsi et al., 2019; Oliphant et al., 2006), we use rainfall to separate the data sample into rainy and dry days keeping in mind the connection of our stochastic description of attenuation with the family of stochastic models of (Rodríguez-Iturbe and Porporato, 2004) and others. This way, bimodal distributions of c ~~shows lower autocorrelations than~~ and k ~~for all the lags analyzed, indicating that the air mass of the atmosphere has seasonality,~~ vanish in most of the cases when data are divided into rainy and dry days, reinforcing the idea that the modes are strongly related to clear and overcast skies conditions. Exceptions to this pattern occur in AT-Neu (Fig. 4), DE-Geb, and DE-Hai, where the PDFs of dry days still have a bimodal distribution.

Results suggest the occurrence of the three PDF types described in section 4. Our interpretation is that a general bimodal-shaped PDF could explain the three types. Following the nomenclature used in the ecohydrological models of (Rodríguez-Iturbe and Porporato, 200 and collaborators (e.g. Tamea et al., 2011; Laio et al., 2009; Nordbotten et al., 2007; Manzoni et al., 2004; Porporato et al., 2003) , let λ be the probability of occurrence a rainy day. Let also x represent any of our indices c and k~~does not manage to remove it.~~ . The PDF of x can then be written as in Eq. (9).

~~By locating the 28 sites analyzed on the Holdridge life zones scheme (see Fig. 6) , we noticed that the geographical location and climate greatly influence the statistical behavior~~

$$f(x) = \lambda f_R(x) + (1-\lambda) f_D(x) \tag{9}$$

where $f_R(x)$ and $f_D(x)$ are the conditional PDF of x for rainy and dry days respectively. The family of this PDFs shown in Figure 7 has members with one and two modes. The UHD-type PDF emerges in the marginal function $f(x)$ when the two modes of $f_R(x)$ and $f_D(x)$ are close to each other.

The general model of Eq. (9) is also useful to understand the climate influence on the marginal PDF of c and k. ~~High latitudes sitesexhibit bimodal distributions, arid to subhumid climates exhibit unimodal distributions with high dispersion,~~ If $\lambda \to 0$ (i.e. in very dry sites) the c and ~~humid tropical regions exhibit unimodal distributions with low dispersion~~k PDFs are of the ULD-type, and are the result of solar geometry and the permanent constituents of the atmosphere. If λ is not so low, the PDF will be of the UHD-type where convection is the main driver of cloud formation and of the B-type where cloud dynamics is controlled by larger-scale phenomena as atmospheric jets and meteorological fronts (Boucher et al., 2013). Obviously, as $\lambda \to 1$ the c and k PDFs will approximate those of the humid days, no matter the physical mechanisms behind.

~~As rainfall is a proxy of cloudiness and water vapor, bimodal distributions vanish when data are divided into rainy and dry days, corroborating that each mode is related to clear and overcast skies conditions (Tovar-Pescador, 2008; Olseth and Skartveit, 1984) .~~

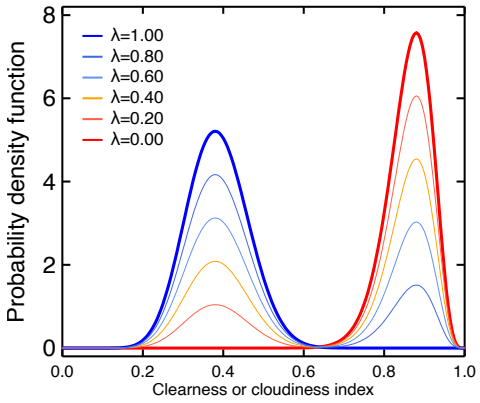

Figure 7. A family of PDFs from the general model of Eq. (9).

~~On the seasonality, we found a clear definition of indices seasons at extratropical sites, unlike tropical sites where local conditions play a determining role. Variations in~~

5.1 Regionalization

As shown in Table 2 and Figure 5, latitude and global climate regions have a weak relation with the PDF types., with ULD occurring in the Tropical, Warm Tropical, Subtropical and Cool temperate regions, UHD in tropical ans subtropical regions, and B-type PDFS in Warm Tropical, Subtropical, Cool temperate regions and boreal regions. There is also one UHD site in the Subpolar region and two ULD in the Polar region. In summary, there is no clear pattern of PDF type variability when grouped by latitude or global climate regions.

The Köppen classification system performs better than global climate regions to capture the PDF type variability (Figure **??**). C climates (Cfa, Cfb, Csa) and Df climates (Dfb and Dfc) have a clear predominance of the ~~beginning and end of indices seasons do not show a notorious spatial pattern . In fact, it is possible to see different behaviors in a similar geographical location, as at the two sites in Belgium. This also can be attributed to local conditions.~~

~~The results obtained in this analysis are useful in a large number of study areas, such as those related to ecohydrology,~~ B-type PDFs, with the exception of one site in Australia (AU-Tum). B climates (BSh and BSk) and Aw climates (with one exception) are all of the ULD type. Am climate is UHD, and a variety of PDF types occurs in the Dwb and Dwc climates.

Plotting the sites on the Holdridge life zones scheme (see Fig. 6) reveals a clear-cut pattern of c and k PDF types. The Holdridge life zones triangle has the advantage of showing several climate variables in an independent way. These variables are humidity, annual precipitation and potential evapotranspiration ratio. Boreal and cool temperate regions in the more humid provinces have PDFs of the B type, tropical regions in the humid provinces show PDFs of the UHD type, and the dry provinces show all ULD-type PDFS. Two isolated sites occur at the top of the triangle, two ULD sites in the polar desert of China and one UHD site in Alaska (see map in Figure 1).

6 Conclusions

We inspected 37 sites worldwide for the influence of local climate on statistical properties of clearness and clear-day indices. We identified three types statistical behavior according to the PDF shape, namely ULD, UHD and B. The same PDF type was found to occur for c and k at each site for both PAR and WS radiation bands. It was evidenced that latitude is not enough to explain the shape of the PDFs, suggesting that climate could play an important role. Global climate region and the Köppen climate have a stronger relation than latitude with the PDF types. Holdridge life zones classification showed the most clear-cut pattern of variability of the PDF types. We proposed a general mathematical model for the PDF of c or k that has the ULD, UHD and B types as particular cases. These model constitutes an important basis for biogeochemical modeling in energy-limited ecosystems, especially in the field of ecohydrology, but also in meteorology, glaciology, agroclimatology ~~, etc. Furthermore, this methodology can be extended to any site and any radiation wavelengths range between 0.5~~ and ~~1991.5 nm~~other research fields.

Author contributions. EM and AO conceived the idea. AO calculated the clear-sky daily radiation. EM did all the statistics. Both EM and AO analyzed the results and wrote the manuscript. AO supervised the work.

Acknowledgements. We thank Departamento Administrativo de Ciencia, Tecnología e Investigación de Colombia (Colciencias) and Universidad Nacional de Colombia for financial support through the programs "Becas de Doctorado Nacionales" ~~program, and the~~ and "Convocatoria para el Apoyo al Desarrollo de Tesis de Posgrado de la Universidad Nacional de Colombia 2018", respectively. ~~This work used data acquired and shared by~~ We also acknowledge the FLUXNET community and the SOLID Project for sharing the data we used in this study.

References

Allen, R. G., Trezza, R., and Tasumi, M.: Analytical integrated functions for daily solar radiation on slopes, Agricultural and Forest Meteorology, 139, 55–73, https://doi.org/10.1016/j.agrformet.2006.05.012, 2006.

Assunção, H. F., Escobedo, J. F., and Oliveira, A. P.: Modelling frequency distributions of 5 minute-averaged solar radiation indexes using Beta probability functions, Theoretical and Applied Climatology, 75, 213–224, https://doi.org/10.1007/s00704-003-0733-9, 2003.

Baldocchi, D., Falge, E., Gu, L., Olson, R., Hollinger, D., Running, S., Anthoni, P., Bernhofer, C., Davis, K., Evans, R., Fuentes, J., Goldstein, A., Katul, G., Law, B., Lee, X., Malhi, Y., Meyers, T., Munger, W., Oechel, W., Paw, K. T., Pilegaard, K., Schmid, H. P., Valentini, R., Verma, S., Vesala, T., Wilson, K., and Wofsy, S.: FLUXNET: A New Tool to Study the Temporal and Spatial Variability of Ecosystem–Scale Carbon Dioxide, Water Vapor, and Energy Flux Densities, Bulletin of the American Meteorological Society, 82, 2415–2434, https://doi.org/10.1175/1520-0477(2001)082<2415:FANTTS>2.3.CO;2, 2001.

Bendt, P., Collares-Pereira, M., and Rabl, A.: The frequency distribution of daily insolation values, Solar Energy, 27, 1–5, https://doi.org/10.1016/0038-092X(81)90013-X, 1981.

Botter, G., Porporato, A., Rodriguez-Iturbe, I., and Rinaldo, A.: Basin-scale soil moisture dynamics and the probabilistic characterization of carrier hydrologic flows: Slow, leaching-prone components of the hydrologic response, Water Resources Research, 43, https://doi.org/10.1029/2006WR005043, http://doi.wiley.com/10.1029/2006WR005043, 2007.

Botter, G., Zanardo, S., Porporato, A., Rodriguez-Iturbe, I., and Rinaldo, A.: Ecohydrological model of flow duration curves and annual minima, Water Resources Research, 44, https://doi.org/10.1029/2008WR006814, http://doi.wiley.com/10.1029/2008WR006814, 2008.

Boucher, O., Randall, D., Artaxo, P., Bretherton, C., Feingold, G., Forster, P., Kerminen, V.-M., Kondo, Y., Liao, H., Lohmann, U., Rasch, P., Satheesh, S., Sherwood, S., Stevens, B., and Zhang, X.: Clouds and Aerosols, in: Climate Change 2013: The Physical Science Basis. Contribution of Working Group I to the Fifth Assessment Report of the Intergovernmental Panel on Climate Change, edited by Stocker, T., Qin, D., Plattner, G.-K., Tignor, M., Allen, S., Boschung, J., Nauels, A., Xia, Y., Bex, V., and Midgley, P., pp. 571–657, Cambridge University Press, Cambridge, United Kingdom and New York, NY, USA, 2013.

Cañada, J., Pedros, G., and Bosca, J.: Relationships between UV (0.290–0.385 μm) and broad band solar radiation hourly values in Valencia and Córdoba, Spain, Energy, 28, 199–217, 2003.

Ceola, S., Botter, G., Bertuzzo, E., Porporato, A., Rodriguez-Iturbe, I., and Rinaldo, A.: Comparative study of ecohydrological streamflow probability distributions, Water Resources Research, 46, https://doi.org/10.1029/2010WR009102, http://doi.wiley.com/10.1029/2010WR009102, 2010.

Chen, T., Rossow, W. B., and Zhang, Y.: Radiative Effects of Cloud-Type Variations, Journal of Climate, 13, 264–286, https://doi.org/10.1175/1520-0442(2000)013<0264:REOCTV>2.0.CO;2, http://journals.ametsoc.org/doi/abs/10.1175/1520-0442{%}282000{%}29013{%}3C0264{%}3AREOCTV{%}3E2.0.CO{%}3B2, 2000.

Daly, E., Porporato, A., and Rodríguez-Iturbe, I.: Coupled Dynamics of Photosynthesis, Transpiration, and Soil Water Balance. Part I: Upscaling from Hourly to Daily Level, Journal of Hydrometeorology, 5, 546–558, https://doi.org/10.1175/1525-7541(2004)005<0546:CDOPTA>2.0.CO;2, http://journals.ametsoc.org/doi/abs/10.1175/1525-7541{%}282004{%}29005{%}3C0546{%}3ACDOPTA{%}3E2.0.CO{%}3B2, 2004a.

Daly, E., Porporato, A., and Rodríguez-Iturbe, I.: Coupled Dynamics of Photosynthesis, Transpiration, and Soil Water Balance. Part II: Stochastic Analysis and Ecohydrological Significance, Journal of Hydrometeorology, 5, 559–

566, https://doi.org/10.1175/1525-7541(2004)005<0559:CDOPTA>2.0.CO;2, http://journals.ametsoc.org/doi/abs/10.1175/1525-7541{%}25282004{%}2529005{%}253C0559{%}253ACDOPTA{%}253E2.0.CO{%}253B2, 2004b.

Dodge, Y.: The Concise Encyclopedia of Statistics, Springer New York, New York, NY, https://doi.org/10.1007/978-0-387-32833-1, 2008.

D'Odorico, P., Ridolfi, L., Porporato, A., and Rodríguez-Iturbe, I.: Preferential states of seasonal soil moisture: The impact of climate fluctuations, Water Resources Research, 36, 2209–2219, https://doi.org/10.1029/2000WR900103, 2000.

D'Odorico, P., Laio, F., Porporato, A., and Rodriguez-Iturbe, I.: Hydrologic controls on soil carbon and nitrogen cycles. II. A case study, Advances in Water Resources, 26, 59–70, https://doi.org/10.1016/S0309-1708(02)00095-7, https://linkinghub.elsevier.com/retrieve/pii/S0309170802000957, 2003.

Engerer, N. A. and Mills, F. P.: KPV: A clear-sky index for photovoltaics, Solar Energy, 105, 679–693, 2014.

Escobedo, J. F., Gomes, E. N., Oliveira, A. P., and Soares, J.: Modeling hourly and daily fractions of UV, PAR and NIR to global solar radiation under various sky conditions at Botucatu, Brazil, Applied Energy, 86, 299–309, https://doi.org/10.1016/j.apenergy.2008.04.013, 2009.

Fernández-Illescas, C. P. and Rodríguez-Iturbe, I.: Hydrologically Driven Hierarchical Competition-Colonization Models: The Impact of Interannual Climate Fluctuations, Ecological Monographs, 73, 207–222, https://doi.org/10.1890/0012-9615(2003)073[0207:HDHCMT]2.0.CO;2, 2003.

Gatto, M., Mari, L., Bertuzzo, E., Casagrandi, R., Righetto, L., Rodríguez-Iturbe, I., and Rinaldo, A.: Spatially explicit conditions for waterborne pathogen invasion, The American Naturalist, 182, 328–46, https://doi.org/10.1086/671258, http://www.ncbi.nlm.nih.gov/pubmed/23933724, 2013.

Gordon, J. M. and Hochman, M.: On the random nature of solar radiation, Solar Energy, 32, 337–342, https://doi.org/10.1016/0038-092X(84)90276-7, 1984.

Haberreiter, M., Schöll, M., Dudok de Wit, T., Kretzschmar, M., Misios, S., Tourpali, K., and Schmutz, W.: A new observational solar irradiance composite, Journal of Geophysical Research: Space Physics, 122, 5910–5930, https://doi.org/10.1002/2016JA023492, 2017.

Hansen, J. W.: Stochastic daily solar irradiance for biological modeling applications, Agricultural and Forest Meteorology, 94, 53–63, https://doi.org/10.1016/S0168-1923(99)00003-9, 1999.

Harrouni, S.: Fractal Classification of Typical Meteorological Days from Global Solar Irradiance: Application to Five Sites of Different Climates, in: Modeling Solar Radiation at the Earth's Surface, edited by Badescu, V., chap. 2, pp. 29–55, Springer-Verlag Berlin Heidelberg, 2008.

Holdridge, L. R.: Determination of World Plant Formations From Simple Climatic Data, Science, 105, 367–368, https://doi.org/10.1126/science.105.2727.367, 1947.

Holdridge, L. R.: Life zone ecology, Tropical Science Center, San Jose, Costa Rica, 1967.

Hollands, K. G. T. and Suehrcke, H.: A three-state model for the probability distribution of instantaneous solar radiation, with applications, Solar Energy, 96, 103–112, https://doi.org/10.1016/j.solener.2013.07.007, 2013.

Ianetz, A. and Kudish, A.: A method for determining the solar global and defining the diffuse and beam irradiation on a clear day, in: Modeling Solar Radiation at the Earth's Surface: Recent Advances, edited by Badescu, V., chap. 4, pp. 93–113, Springer-Verlag Berlin Heidelberg, https://doi.org/10.1007/978-3-540-77455-6_4, 2008.

Ibánez, M., Rosell, J. I., and Beckman, W. A.: A bi-variable probability density function for the daily clearness index, Solar Energy, 75, 73–80, 2003.

Iqbal, M.: An Introduction to Solar Radiation, Academic Press, Toronto, 1983.

Jurado, M., Caridad, J. M., and Ruiz, V.: Statistical distribution of the clearness index with radiation data integrated over five minute intervals, Solar energy, 55, 469–473, https://doi.org/10.1016/0038-092X(95)00067-2, 1995.

Kasten, F. and Young, A. T.: Revised optical air mass tables and approximation formula, Applied Optics, 28, 4735, https://doi.org/10.1364/AO.28.004735, 1989.

Laio, F., Porporato, A., Ridolfi, L., and Rodríguez-Iturbe, I.: Plants in water-controlled ecosystems: active role in hydrologic processes and response to water stress II. Probabilistic soil moisture dynamics, Advances in Water Resources, 24, 707–723, https://doi.org/10.1016/S0309-1708(01)00005-7, http://linkinghub.elsevier.com/retrieve/pii/S0309170801000057, 2001.

Laio, F., Tamea, S., Ridolfi, L., D'Odorico, P., and Rodríguez-Iturbe, I.: Ecohydrology of groundwater-dependent ecosystems: 1. Stochastic water table dynamics, Water Resources Research, 45, 1–13, https://doi.org/10.1029/2008WR007292, 2009.

Leckner, B.: The spectral distribution of solar radiation at the earth's surface—elements of a model, Solar Energy, 20, 143–150, https://doi.org/10.1016/0038-092X(78)90187-1, 1978.

Leemans, R.: Global Holdridge Life Zone Classifications, Digital Raster Data, in: Global Ecosystems Database Version 2.0, NOAA National Geophysical Data Center, Boulder, USA, 1992.

Li, Z. and Trishchenko, A. P.: Quantifying Uncertainties in Determining SW Cloud Radiative Forcing and Cloud Absorption due to Variability in Atmospheric Conditions, Journal of the Atmospheric Sciences, 58, 376–389, https://doi.org/10.1175/1520-0469(2001)058<0376:QUIDSC>2.0.CO;2, http://journals.ametsoc.org/doi/abs/10.1175/1520-0469{%}282001{%}29058{%}3C0376{%}3AQUIDSC{%}3E2.0.CO{%}3B2, 2001.

Liu, B. Y. and Jordan, R. C.: The interrelationship and characteristic distribution of direct, diffuse and total solar radiation, Solar Energy, 4, 1–19, https://doi.org/10.1016/0038-092X(60)90062-1, 1960.

Manzoni, S., Porporato, A., D'Odorico, P., Laio, F., and Rodriguez-Iturbe, I.: Soil nutrient cycles as a nonlinear dynamical system, Nonlinear Processes in Geophysics, 11, 589–598, https://doi.org/10.5194/npg-11-589-2004, 2004.

Martinez-Lozano, J. A., Tena, F., and Utrillas, M. P.: Ratio of UV to global broad band irradiation in Valencia, Spain, International Journal of Climatology, 19, 903–911, 1999.

Mercado, L. M., Bellouin, N., Sitch, S., Boucher, O., Huntingford, C., Wild, M., and Cox, P. M.: Impact of changes in diffuse radiation on the global land carbon sink, Nature, 458, 1014–1017, https://doi.org/10.1038/nature07949, http://www.nature.com/doifinder/10.1038/nature07949, 2009.

Muñoz, E., Ochoa, A., and Cordão-Neto, M.: Stochastic ecohydrological-geotechnical modeling of long-term slope stability, Landslides, 15, 913–924, https://doi.org/10.1007/s10346-017-0923-7, http://link.springer.com/10.1007/s10346-017-0923-7, 2018.

Muñoz, E., Ochoa, A., Poveda, G., and Rodríguez-Iturbe, I.: Probabilistic soil moisture dynamics of water- and energy-limited ecosystems, EarthArXiv, https://doi.org/10.31223/osf.io/au4tb, https://eartharxiv.org/au4tb/, 2020.

NASA: U.S. Standard Atmosphere, 1976, Tech. rep., NOAA, Washington, D.C., 1976.

Nordbotten, J. M., Rodriguez-Iturbe, I., and Celia, M. A.: Stochastic coupling of rainfall and biomass dynamics, Water Resources Research, 43, 1–7, https://doi.org/10.1029/2006WR005068, 2007.

Nyamsi, W. W., Blanc, P., Augustine, J. A., Arola, A., and Wald, L.: A new clear-sky method for assessing photosynthetically active radiation at the surface level, Atmosphere, 10, https://doi.org/10.3390/ATMOS10040219, 2019.

Oliphant, A., Susan, C., Grimmond, B., Schmid, H. P., and Wayson, C. A.: Local-scale heterogeneity of photosynthetically active radiation (PAR), absorbed PAR and net radiation as a function of topography, sky conditions and leaf area index, Remote Sensing of Environment, 103, 324–337, https://doi.org/10.1016/j.rse.2005.09.021, 2006.

Olseth, J. A. and Skartveit, A.: A probability density function for daily insolation within the temperate storm belts, Solar Energy, 33, 533–542, https://doi.org/10.1016/0038-092X(84)90008-2, 1984.

Olson, R., Holladay, S., Cook, R., Falge, E., Baldocchi, D., and Gu, L.: FLUXNET. Database of fluxes, site characteristics, and flux-community information, Tech. rep., Oak Ridge National Laboratory (ORNL), Oak Ridge, TN (United States), https://doi.org/10.2172/1184413, 2004.

Pearson, K.: X. On the criterion that a given system of deviations from the probable in the case of a correlated system of variables is such that it can be reasonably supposed to have arisen from random sampling, The London, Edinburgh, and Dublin Philosophical Magazine and Journal of Science, 50, 157–175, https://doi.org/10.1080/14786440009463897, 1900.

Peel, M., Finlayson, B., and McMahon, T.: Updated world map of the Köppen-Geiger climate classification, Hydrology and Earth System Sciences, 11, 1633–1644, https://doi.org/10.5194/hess-11-1633-2007, http://www.hydrol-earth-syst-sci.net/11/1633/2007/, 2007.

Platt, U., Pfeilsticker, K., and Vollmer, M.: Radiation and Optics in the Atmosphere, in: Springer Handbook of Lasers and Optics, edited by Träger, F., pp. 1475–1517, Springer Berlin Heidelberg, Berlin, Heidelberg, https://doi.org/10.1007/978-3-642-19409-2_23, http://link.springer.com/10.1007/978-3-642-19409-2{_}23, 2012.

Polo, J., Zarzalejo, L., and Ramírez, L.: Solar Radiation Derived from Satellite Images, in: Modeling Solar Radiation at the Earth's Surface, edited by Badescu, V., chap. 18, pp. 449–461, Springer-Verlag Berlin Heidelberg, 2008.

Porporato, A., Laio, F., Ridolfi, L., and Rodríguez-Iturbe, I.: Plants in water-controlled ecosystems: active role in hydrologic processes and response to water stress III. Vegetation water stress, Advances in Water Resources, 24, 725–744, https://doi.org/10.1016/S0309-1708(01)00006-9, http://linkinghub.elsevier.com/retrieve/pii/S0309170801000069, 2001.

Porporato, A., D'Odorico, P., Laio, F., Ridolfi, L., and Rodríguez-Iturbe, I.: Ecohydrology of water-controlled ecosystems, Advances in Water Resources, 25, 1335–1348, https://doi.org/10.1016/S0309-1708(02)00058-1, http://linkinghub.elsevier.com/retrieve/pii/S0309170802000581, 2002.

Porporato, A., D'Odorico, P., Laio, F., and Rodriguez-Iturbe, I.: Hydrologic controls on soil carbon and nitrogen cycles. I. Modeling scheme, Advances in Water Resources, 26, 45–58, https://doi.org/10.1016/S0309-1708(02)00094-5, 2003.

Ridolfi, L., D'Odorico, P., Porporato, A., and Rodriguez-Iturbe, I.: Impact of climate variability on the vegetation water stress, Journal of Geophysical Research: Atmospheres, 105, 18 013–18 025, https://doi.org/10.1029/2000JD900206, http://doi.wiley.com/10.1029/2000JD900206, 2000.

Ridolfi, L., D'Odorico, P., Porporato, A., and Rodriguez-Iturbe, I.: The influence of stochastic soil moisture dynamics on gaseous emissions of NO, N2O, and N2, Hydrological Sciences Journal, 48, 781–798, https://doi.org/10.1623/hysj.48.5.781.51451, https://www.tandfonline.com/doi/abs/10.1623/hysj.48.5.781.51451, 2003.

Ridolfi, L., D'Odorico, P., Laio, F., Tamea, S., and Rodriguez-Iturbe, I.: Coupled stochastic dynamics of water table and soil moisture in bare soil conditions, Water Resources Research, 44, 1–11, https://doi.org/10.1029/2007WR006707, 2008.

Robinson, N.: Solar Radiation, Elsevier, Amsterdam, 1966.

Rodríguez-Iturbe, I. and Porporato, A.: Ecohydrology of Water-Controlled Ecosystems, Cambridge University Press, USA, 2004.

Rodríguez-Iturbe, I., D'Odorico, P., Porporato, A., and Ridolfi, L.: On the spatial and temporal links between vegetation, climate, and soil moisture, Water Resources Research, 35, 3709–3722, https://doi.org/10.1029/1999WR900255, http://www.agu.org/pubs/crossref/1999/1999WR900255.shtml, 1999a.

Rodríguez-Iturbe, I., Porporato, A., Ridolfi, L., Isham, V., and Cox, D.: Probabilistic modelling of water balance at a point: the role of climate, soil and vegetation, Proceedings of the Royal Society A: Mathematical, Physical and Engineering Sciences, 455, 3789–3805, https://doi.org/10.1098/rspa.1999.0477, http://rspa.royalsocietypublishing.org/cgi/doi/10.1098/rspa.1999.0477, 1999b.

Rodríguez-Iturbe, I., Porporato, A., Laio, F., and Ridolfi, L.: Plants in water-controlled ecosystems: active role in hydrologic processes and response to water stress I. Scope and general outline, Advances in Water Resources, 24, 695–705, https://doi.org/10.1016/S0309-1708(01)00004-5, http://linkinghub.elsevier.com/retrieve/pii/S0309170801000045, 2001.

Rubel, F. and Kottek, M.: Observed and projected climate shifts 1901-2100 depicted by world maps of the Köppen-Geiger climate classification, Meteorologische Zeitschrift, 19, 135–141, https://doi.org/10.1127/0941-2948/2010/0430, 2010.

Sager, J. C. and McFarlane, J. C.: Radiation, in: Growth Chamber Handbook, edited by Langhans, R. and Tibbitts, T., pp. 1–30, NC-101 Committee on Controlled Environment Technology and Use, 1997.

Schaffer, B. E., Nordbotten, J. M., and Rodriguez-Iturbe, I.: Plant biomass and soil moisture dynamics: analytical results, Proceedings of the Royal Society A: Mathematical, Physical and Engineering Science, 471, 20150 179, https://doi.org/10.1098/rspa.2015.0179, http://rspa.royalsocietypublishing.org/lookup/doi/10.1098/rspa.2015.0179, 2015.

Schöll, M., Dudok de Wit, T., Kretzschmar, M., and Haberreiter, M.: Making of a solar spectral irradiance dataset I: observations, uncertainties, and methods, Journal of Space Weather and Space Climate, 6, https://doi.org/10.1051/swsc/2016007, 2016.

Scholz, F. and Stephens, M.: K-Sample Anderson-Darling Tests, Journal of the Amerlcan Statistical Association, 82, 918–924, https://doi.org/10.2307/2288805, 1987.

Skartveit, A. and Olseth, J. A.: The probability density and autocorrelation of short-term global and beam irradiance, Solar Energy, 49, 477–487, https://doi.org/10.1016/0038-092X(92)90155-4, 1992.

Tamea, S., Laio, F., Ridolfi, L., D'Odorico, P., and Rodriguez-Iturbe, I.: Ecohydrology of groundwater-dependent ecosystems: 2. Stochastic soil moisture dynamics, Water Resources Research, 45, https://doi.org/10.1029/2008WR007293, http://doi.wiley.com/10.1029/2008WR007293, 2009.

Tamea, S., Laio, F., Ridolfi, L., and Rodriguez-Iturbe, I.: Crossing properties for geophysical systems forced by Poisson noise, Geophysical Research Letters, 38, 1–5, https://doi.org/10.1029/2011GL049074, 2011.

Thompson, S., Levin, S., and Rodríguez-Iturbe, I.: Linking plant disease risk and precipitation drivers: a dynamical systems framework, The American Naturalist, 181, E1–16, https://doi.org/10.1086/668572, http://www.ncbi.nlm.nih.gov/pubmed/23234853, 2013.

Tovar-Pescador, J.: Modelling the statistical properties of solar radiation and proposal of a technique based on Boltzmann statistics, in: Modeling Solar Radiation at the Earth's Surface: Recent Advances, edited by Badescu, V., chap. 3, pp. 55–91, Springer-Verlag Berlin Heidelberg, https://doi.org/10.1007/978-3-540-77455-6_3, 2008.

Tran, V. L.: Stochastic models of solar radiation processes, Ph.D. thesis, Université d'Orléans, 2013.

Utrillas, M. P., Marín, M. J., Esteve, A. R., Salazar, G., Suárez, H., Gandía, S., and Martínez-Lozano, J. A.: Relationship between erythemal UV and broadband solar irradiation at high altitude in Northwestern Argentina, Energy, 162, 136–147, 2018.

Vigroux, E.: Contribution à l'étude expérimentale de l'absorption de l'ozone, Annales de Physique, 12, 709–762, https://doi.org/10.1051/anphys/195312080709, 1953.

Wallace, J. M. and Hobbs, P. V.: Atmospheric Science. An Introductory Survey, Academic Press, 2 edn., 2006.

Wu, A., Song, Y., van Oosterom, E. J., and Hammer, G. L.: Connecting Biochemical Photosynthesis Models with Crop Models to Support Crop Improvement, Frontiers in Plant Science, 7, https://doi.org/10.3389/fpls.2016.01518, http://journal.frontiersin.org/article/10.3389/fpls.2016.01518/full, 2016.